INTERNATIONAL JOURNAL FOR NUMERICAL METHODS IN FLUIDS, VOL. 10, 557–568 (1990)

LEAST-SQUARES FINITE ELEMENT METHODS FOR COMPRESSIBLE EULER EQUATIONS

BO-NAN JIANG

Institute for Computational Mechanics in Propulsion, NASA Lewis Research Center, Cleveland, OH 44135, U.S.A.

AND

G. F. CAREY

Computational Fluid Dynamics Laboratory, The University of Texas at Austin, Austin, TX 78712, U.S.A.

SUMMARY

A method based on backward finite differencing in time and a least-squares finite element scheme for first-order systems of partial differential equations in space is applied to the Euler equations for gas dynamics. The scheme minimizes the L^2-norm of the residual within each time step. The method naturally generates numerical dissipation proportional to the time step size. An implicit method employing linear elements has been implemented and proves robust. For high-order elements, computed solutions based on the L^2-method may have oscillations for calculations at similar time step sizes. To overcome this difficulty, a scheme which minimizes the weighted H^1-norm of the residual is proposed and leads to a successful scheme with high-degree elements. Finally, a conservative least-squares finite element method is also developed. Numerical results for two-dimensional problems are given to demonstrate the shock resolution of the methods and compare different approaches.

KEY WORDS Compressible Euler equations Finite element Least-squares method Shock resolution

1. INTRODUCTION

Finite element methods are well suited to practical problems posed on complicated domains and are now extensively applied in solid mechanics, heat transfer, fluid flow and other areas of applied science. The earlier difficulties encountered in extending the methodology beyond elliptic boundary value problems and to convection dominated flows have been substantially resolved. In particular, the success of upwind finite differencing and related artificial dissipation methods motivated studies of analogous upwind finite element methods; similarly, the idea of the Lax–Wendroff scheme in finite differencing has motivated studies of Taylor–Galerkin finite element algorithms. For example, the streamline upwind Petrov–Galerkin method,[1] the Taylor–Galerkin method,[2–4] the Taylor–Galerkin method with flux-corrected transport (FCT),[5–7] block relaxation via Godunov's method[8] and the characteristic Galerkin method[9] have been developed and applied with considerable success to these problems.

In previous studies[10–15] we described a least-squares finite element method (LSFEM) for hyperbolic problems. Here this approach is extended to the Euler equations of compressible gas dynamics. We begin by considering the backward implicit time-differenced formulation. The least-squares method is then employed to minimize the residual in the L^2-norm. This approach

0271–2091/90/050557–12$06.00

Received 29 December 1988
Revised 30 June 1989

yields a weak statement similar to the streamline upwind Petrov–Galerkin scheme. The associated artificial viscosity appears 'naturally' and is dependent on the time step Δt, but without other 'free' parameters. For linear problems the implicit method is unconditionally stable at all Courant numbers.

The application of this L^2-method with linear elements to the compressible Euler equations produces non-oscillatory shock profiles as long as the time step Δt is large enough (Courant numbers in the range 10–50). While this, evidently, is not appropriate for time-accurate solutions, it is a valid approach for the steady shocked flow computation. We also investigate the possibility of utilizing high-degree bases. For high-order elements and moderate time steps the L^2-method may lead to a solution with non-physical oscillations. In order to overcome this difficulty, we construct a new least-squares variational method based on minimizing the residual in an approximate H^1-norm. The effect of the additional term is to introduce a further dissipation proportional to the solution gradient and thereby control non-linear instabilities associated with shock formation. This strategy can be interpreted as a multi-objective programming technique which minimizes the residual as well as the derivatives of the residual. The application of the method to one-dimensional unsteady Euler equations is discussed in Jiang and Carey.[12] One aim of the present paper is to demonstrate its applicability for two-dimensional problems and to develop a successful method using higher-degree elements. For comparison purposes we also present a similar least-squares finite element method based on a conservative formulation.

In Section 2 we give a description of the L^2-method and explain the mechanism of numerical dissipation generated by the method. The H^1-method is discussed in Section 3. In Section 4 we describe the conservative formulation. Numerical examples are given to illustrate the shock-capturing capability of the method.

2. L^2-METHOD

2.1. Formulation

We begin by describing the LSFEM for the two-dimensional unsteady compressible Euler equations in non-conservative form as a first-order system:

$$\frac{\partial \mathbf{u}}{\partial t} + \mathbf{A}_1 \frac{\partial \mathbf{u}}{\partial x} + \mathbf{A}_2 \frac{\partial \mathbf{u}}{\partial y} = \mathbf{0} \qquad \text{in } \Omega \times (0, T), \tag{1}$$

$$\mathbf{M}\mathbf{u} = \mathbf{g} \qquad \text{on } \Gamma_g \times (0, T), \tag{2}$$

$$\mathbf{u} = \mathbf{u}_0 \qquad \text{in } \Omega \text{ for } t = 0, \tag{3}$$

where $\mathbf{u}^T = (\rho, u, v, p)$, $\mathbf{M}$ is a boundary operator, $\mathbf{g}$ is a given vector-valued function, Γ_g is that part of the boundary Γ where essential boundary conditions are applied, Ω is the spatial domain of the problem, t is time and

$$\mathbf{A}_1 = \begin{bmatrix} u & \rho & 0 & 0 \\ 0 & u & 0 & \rho^{-1} \\ 0 & 0 & u & 0 \\ 0 & \gamma p & 0 & u \end{bmatrix}, \qquad \mathbf{A}_2 = \begin{bmatrix} v & 0 & \rho & 0 \\ 0 & v & 0 & 0 \\ 0 & 0 & v & \rho^{-1} \\ 0 & 0 & \gamma p & v \end{bmatrix}.$$

Here ρ is the density, (u, v) are the velocity components, p is the pressure and γ is the specific heat ratio.

For a given time step $\Delta t = t^{n+1} - t^n$ we linearize the problem by setting $\mathbf{A}_1^n = \mathbf{A}_1(\mathbf{u}^n)$, $\mathbf{A}_2^n = \mathbf{A}_2(\mathbf{u}^n)$. Backward differencing leads to the implicit time-differenced problem

$$\mathbf{u}^{n+1} - \mathbf{u}^n + \Delta t \mathbf{A}_1^n \frac{\partial \mathbf{u}^{n+1}}{\partial x} + \Delta t \mathbf{A}_2^n \frac{\partial \mathbf{u}^{n+1}}{\partial y} = \mathbf{0}. \tag{4}$$

Introducing $\Delta \mathbf{u} = \mathbf{u}^{n+1} - \mathbf{u}^n$ we rewrite equation (4) as

$$\Delta \mathbf{u} + \Delta t \mathbf{A}_1^n \frac{\partial \Delta \mathbf{u}}{\partial x} + \Delta t \mathbf{A}_2^n \frac{\partial \Delta \mathbf{u}}{\partial y} + \Delta t \left(\mathbf{A}_1^n \frac{\partial \mathbf{u}^n}{\partial x} + \mathbf{A}_2^n \frac{\partial \mathbf{u}^n}{\partial y} \right) = \mathbf{0}. \tag{5}$$

The basic least-squares method for the system (5) amounts to minimizing the L^2-norm of the residual $\mathbf{R}$ for admissible $\Delta \mathbf{u}$ in (5); i.e. minimizing the objective functional

$$\Phi_0 = \int_\Omega \mathbf{R}^{\mathrm{T}} \mathbf{R} \, \mathrm{d}x\mathrm{d}y, \tag{6}$$

with

$$\mathbf{R} = \left[\Delta \mathbf{u} + \Delta t \mathbf{A}_1^n \frac{\partial \Delta \mathbf{u}}{\partial x} + \Delta t \mathbf{A}_2^n \frac{\partial \Delta \mathbf{u}}{\partial y} + \Delta t \left(\mathbf{A}_1^n \frac{\partial \mathbf{u}^n}{\partial x} + \mathbf{A}_2^n \frac{\partial \mathbf{u}^n}{\partial y} \right) \right].$$

Taking variations with respect to $\Delta \mathbf{u}$ and setting the test function $\mathbf{v} = \delta \Delta \mathbf{u}$, $\delta \Phi_0 = 0$ leads to the least-squares weak statement: find $\Delta \mathbf{u} \in \mathbf{S} = \{H^1(\Omega))^4; \mathbf{M}(\Delta \mathbf{u}) = \mathbf{0} \text{ on } \Gamma_g\}$, where $H^1(\Omega)$ denotes the usual Hilbert space, such that

$$\int_\Omega \left[\mathbf{v} + \Delta t \mathbf{A}_1^n \frac{\partial \mathbf{v}}{\partial x} + \Delta t \mathbf{A}_2^n \frac{\partial \mathbf{v}}{\partial y} \right]^{\mathrm{T}} \left[\Delta \mathbf{u} + \Delta t \mathbf{A}_1^n \frac{\partial \Delta \mathbf{u}}{\partial x} + \Delta t \mathbf{A}_2^n \frac{\partial \Delta \mathbf{u}}{\partial y} + \Delta t \left(\mathbf{A}_1^n \frac{\partial \mathbf{u}^n}{\partial x} + \mathbf{A}_2^n \frac{\partial \mathbf{u}^n}{\partial y} \right) \right] \mathrm{d}x\mathrm{d}y = 0 \quad \forall \, \mathbf{v} \in \mathbf{S}. \tag{7}$$

Next we introduce a finite element discretization. Let N_e be the number of nodes for an element and ψ_j denote the element basis functions. The approximation and the test function are

$$\Delta \mathbf{u}_h(x, y) = \sum_{j=1}^{N_e} \psi_j(x, y) \mathbf{E} \Delta \begin{bmatrix} \rho \\ u \\ v \\ p \end{bmatrix}_j,$$

$$\mathbf{v}_h(x, y) = \psi_i(x, y) \mathbf{E}, \tag{8}$$

where $\Delta(\rho, u, v, p)_j^{\mathrm{T}}$ are the nodal values at the jth node and $\mathbf{E}$ is the 4×4 identity matrix. Substituting $\Delta \mathbf{u}_h$, $\mathbf{v}_h$ for $\Delta \mathbf{u}$, $\mathbf{v}$ in (7) and evaluating the integrals, we have

$$\mathbf{K}(\Delta \mathbf{U}) = \mathbf{F}, \tag{9}$$

where $\Delta \mathbf{U}$ is the global nodal vector. The global matrix $\mathbf{K}$ and the global vector $\mathbf{F}$ are assembled from the following submatrices and subvectors respectively:

$$\mathbf{K}_{ij}^e = \int_{\Omega_e} (\mathbf{L}\psi_i)^{\mathrm{T}} \mathbf{L}\psi_j \, \mathrm{d}x\mathrm{d}y, \tag{10}$$

$$\mathbf{F}_i^e = \int_{\Omega_e} (\mathbf{L}\psi_i)^{\mathrm{T}} \Delta t \left(\mathbf{A}_1^n \frac{\partial \mathbf{u}^n}{\partial x} + \mathbf{A}_2^n \frac{\partial \mathbf{u}^n}{\partial y} \right) \mathrm{d}x\mathrm{d}y, \tag{11}$$

where

$$\mathbf{L}\psi_i = \psi_i \mathbf{E} + \Delta t \psi_{i,x} \mathbf{A}_1^n + \Delta t \psi_{i,y} \mathbf{A}_2^n. \tag{12}$$

We note that the stiffness matrix $\mathbf{K}$ is symmetric, positive and definite. This is an important feature of the least-squares method. Only the lower half matrix need be generated and stored for use in a Cholesky LDL^T factorization.

Remarks: 1. The method presented here is first-order accurate in time. Crank–Nicolson finite differencing in the temporal domain can be introduced to get second-order accuracy (in time). However, for one-dimensional Euler equations the second-order scheme leads to oscillations at shocks (e.g. in computing Sod's problem[12]) and we may anticipate a similar difficulty for two-dimensional problems.

2. In the development above and in the subsequent calculations we use the transient formulation. We remark also that when the steady state is reached by the time-marching procedure, the corresponding weak statement becomes

$$\int_\Omega \left\{ \mathbf{v}^T \left[\mathbf{A}_1 \frac{\partial \mathbf{u}}{\partial x} + \mathbf{A}_2 \frac{\partial \mathbf{u}}{\partial y} \right] + \Delta t \left[\mathbf{A}_1 \frac{\partial \mathbf{v}}{\partial x} + \mathbf{A}_2 \frac{\partial \mathbf{v}}{\partial y} \right]^T \left[\mathbf{A}_1 \frac{\partial \mathbf{u}}{\partial x} + \mathbf{A}_2 \frac{\partial \mathbf{u}}{\partial y} \right] \right\} \mathrm{d}x\mathrm{d}y = \mathbf{0}. \tag{13}$$

The first term in (13) corresponds to the standard Galerkin weak statement. The second term is positive and acts as a numerical dissipation to stabilize the solution, smoothing out any oscillations and discontinuities. (For further discussion on the relationship to the Petrov–Galerkin approach, see Reference 12.)

2.2. *Numerical results*

We now demonstrate some features of the LSFEM using three numerical examples.

Problem 1. A standard test problem corresponding to the reflection of a shock from a wall is depicted in Figure 1. On the upper boundary of the flow domain $\rho = 1{\cdot}7$, $u = 2{\cdot}6185$, $v = -0{\cdot}5082$, $p = 1{\cdot}5282$ and on the upstream boundary $\rho = 1{\cdot}0$, $u = 2{\cdot}9$, $v = 0{\cdot}0$, $p = 0{\cdot}7143$, so a shock emanates from the upper left corner. This shock is reflected at the lower wall where $v = 0$ and the downstream boundary conditions remain free for outflow. The initial data were prescribed as constant at values given on the upper boundary and the specific heat ratio is $\gamma = 1{\cdot}4$. In the calculation a uniform 60×20 mesh of bilinear elements was used. The solution is integrated with a time step $\Delta t = 0{\cdot}333\,33$ until an essentially steady state is obtained in 12 time steps. Pressure contours for this steady solution are given in Figure 1. Qualitatively, it is seen that the flow physics is correctly modelled. Although the shock is somewhat smeared, the results are quite good, oscillations being absent, and the calculation is efficient since the result is achieved in very few steps and the system is symmetric as noted previously.

Problem 2. The second problem is a Mach 3 flow (with $\gamma = 1{\cdot}4$) over a 20° ramp. The gas enters with uniform flow conditions through the left boundary of the domain and an oblique shock develops at the root of the ramp. The mesh contained 824 bilinear elements and the computed pressure contours are illustrated in Figure 2. In the calculation the initial data were prescribed as constant at the value given on the left boundary and the time step was $\Delta t = 0{\cdot}333\,33$. The steady state was obtained in 16 time steps. The present results compare favourably with other calculations reported in the cited references on comparable grids.

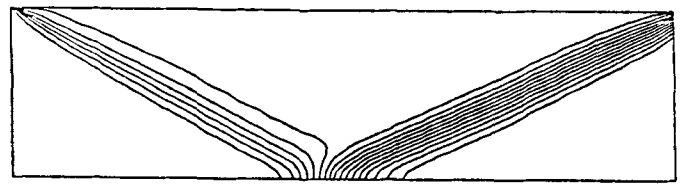

Figure 1. Pressure contours for the wave reflection problem (L^2-method, 20 × 60 bilinear elements, $\Delta t = 0{\cdot}333\,33$, 12 time steps, 2 × 2 Gaussian quadrature)

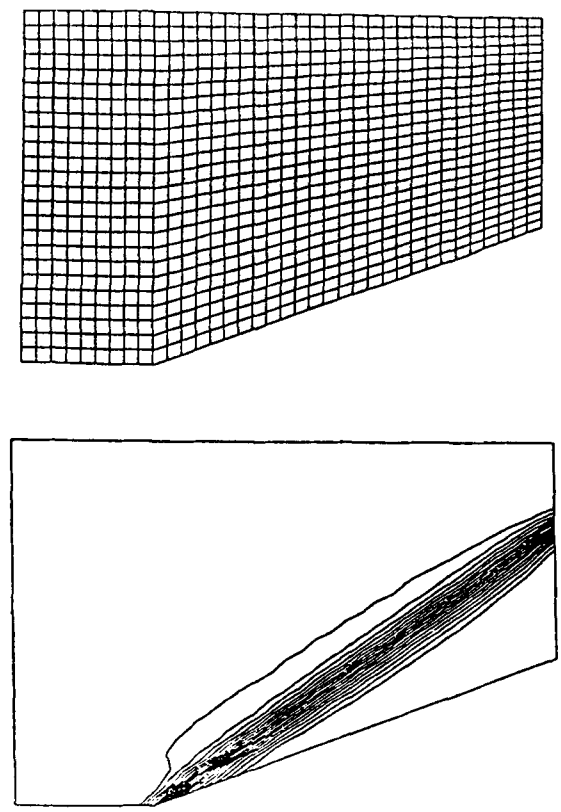

Figure 2. Finite element mesh and pressure contours for the Mach 3 flow over a 20° ramp (L^2-method, 824 bilinear elements, $\Delta t = 0{\cdot}333\,33$, 16 time steps)

Problem 3. We also considered a cylinder in a supersonic flow with Mach number $M_\infty = 2$, $\gamma = 1{\cdot}40$. The mesh of 800 bilinear elements and the computed pressure contours are given in Figure 3. In the calculation the initial data were again prescribed as constant at the value of the incoming flow. The steady state was obtained in 36 time steps with $\Delta t = 0{\cdot}1$.

We note that in all three numerical examples this least-squares finite element method with bilinear elements produces non-oscillatory shock profiles and the results compare favourably with those in the literature based on other methods.

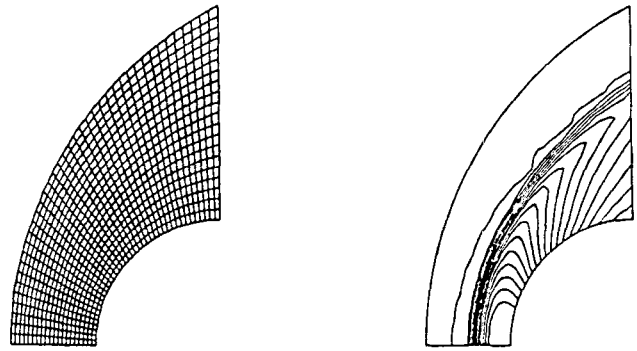

Figure 3. Finite element mesh and pressure contours for the Mach 2 flow past a circular cylinder (L^2-method, 800 bilinear elements, $\Delta t = 0{\cdot}1$, 36 time steps)

3. H^1-METHOD

3.1. Formulation

Numerical experiments show that as long as the time step Δt is large enough (the corresponding Courant number is in the approximate range 10–50), the L^2-method with linear elements gives non-oscillatory shock profiles in the computed steady state. However, for high-order elements, computed solutions based on this method may have oscillations. Moreover, the steepening shock may lead to non-linear instabilities in the calculation. This difficulty is common to present numerical schemes for this type of problem and various dissipation schemes have been introduced to stabilize the results. To circumvent this problem we could modify the objective function to control the residual derivatives. Consider, for example, the following multi-objective optimization problem: minimize the modified functional

$$\Phi = \int_\Omega \left\{ \mathbf{R}^2 + \beta \left[\left(\frac{\partial \mathbf{R}}{\partial x} \right)^2 + \left(\frac{\partial \mathbf{R}}{\partial y} \right)^2 \right] \right\} \mathrm{d}x\mathrm{d}y, \tag{14}$$

where β is a small parameter, $0 < \beta \ll 1$. The effect of the additional term will be to control local non-linear instabilities associated with shock development where large changes in the residual occur. Note that minimizing the functional (14) can be interpreted as minimizing the weighted H^1-norm of $\mathbf{R}$. However, the form in (14) contains second derivatives of $\mathbf{u}$, which implies that, for conformity, C^1-elements are appropriate. Generally, for two- and three-dimensional problems, simpler elements are desirable. An alternative formulation based on (14) can be constructed using high-order elements in a C^0-method. That is, instead of (14) the same goal can be achieved by defining

$$\Phi = \sum_{e=1}^{N} \Phi_e, \tag{15}$$

where N is the number of elements and

$$\Phi_e = \int_{\Omega_e} \left\{ \mathbf{R}^2 + \beta \left[\left(\frac{\partial \mathbf{R}}{\partial x} \right)^2 + \left(\frac{\partial \mathbf{R}}{\partial y} \right)^2 \right] \right\} \mathrm{d}x\mathrm{d}y. \tag{16}$$

That is, the added functional is defined on the element interiors and, using for instance quadratic or cubic C^0-elements, the contributions of the second derivatives in the element interiors can be calculated for (16).

3.2. Numerical results

We now demonstrate the shock-capturing ability of the H^1-LSFEM using the shock wave reflection problem in Section 2.2 (Problem 1). In the calculation, uniform 20×5 meshes with 8-node isoparametric quadratic elements, 9-node biquadratic elements and 12-node isoparametric cubic elements are considered. The solution is integrated with a time step $\Delta t = 0{\cdot}5$ until an essentially steady state is obtained. Pressure contours with the L^2-method and the H^1-method for this steady solution are given for comparison in Figures 4–7 for calculations with each high-order element type indicated above. For calculations with the L^2-method there are a few small oscillations in the pressure solution, seen as 'islands' in the contour plots. These oscillations are suppressed without degrading solution accuracy by setting β to a small value. Results for $\beta = 10^{-6}$ are shown in successive plots and confirm this behaviour. The results appear relatively insensitive to β (e.g. see Reference 12).

Figures 5 and 6 show the pressure contours for the same problem at different time steps. When the number of time steps increases from 7 to 10, the results of the H^1-method remain stable but those for the L^2-method have more 'islands'. Similar results are seen in Figure 7 for cubic elements, which do not appear to offer any advantage over quadratic elements since the accuracy is also controlled by the time increment Δt and the time integration is of low order, $O(\Delta t)$. In a time-accurate calculation with a sufficiently small time step, some benefit from very-high-degree elements may be possible, but the practicality of such an approach is arguable. The pressure contours for quadratic elements and smaller step size are shown in Figure 8. Comparing the contours in Figure 8 with those in Figure 1, it is observed that the shock is captured better by using quadratic elements than with linear elements and there is little smearing even though the grid is quite coarse. Hence quadratic elements are quite effective.

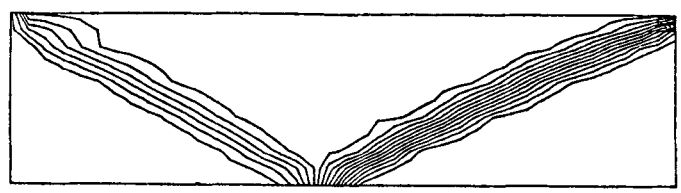

a. L^2 method

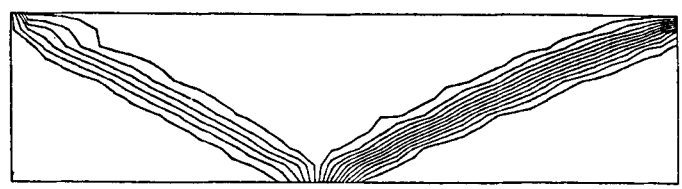

b. H^1 method

Figure 4. Pressure contours for the wave reflection problem (5×20 8-node quadratic elements, $\Delta t = 0{\cdot}5$, 8 time steps, 2×2 Gaussian quadrature)

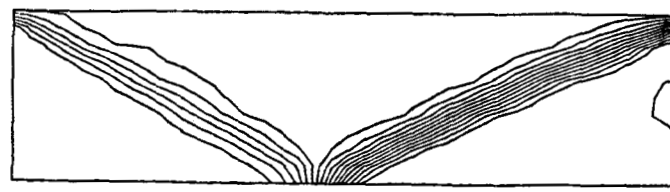

a. L^2 method

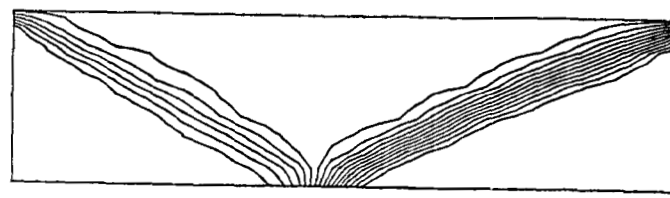

b. H^1 method

Figure 5. Pressure contours for the wave reflection problem (5 × 20 9-node quadratic elements, $\Delta t = 0{\cdot}5$, 7 time steps, 3 × 3 Gaussian quadrature)

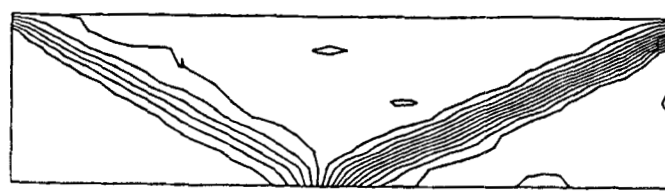

a. L^2 method

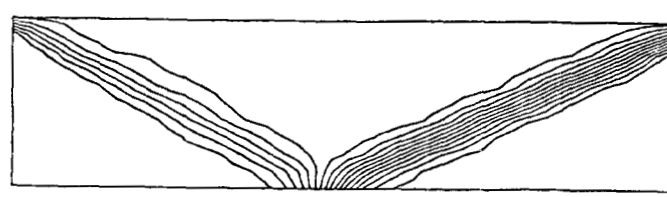

b. H^1 method

Figure 6. Pressure contours for the wave reflection problem (5 × 20 8-node quadratic elements, $\Delta t = 0{\cdot}5$, 10 time steps, 3 × 3 Gaussian quadrature)

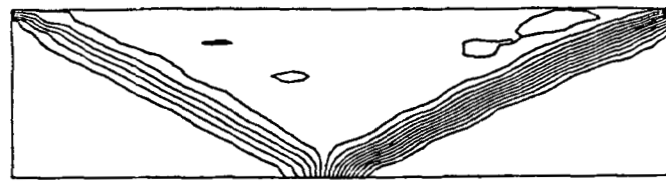

a. L^2 method

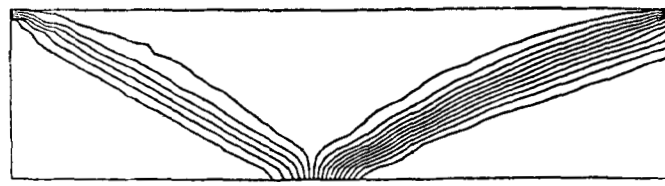

b. H^1 method

Figure 7. Pressure contours for the wave reflection problem (5×20 12-node cubic elements, $\Delta t = 0{\cdot}5$, 8 time steps, 3×3 Gaussian quadrature)

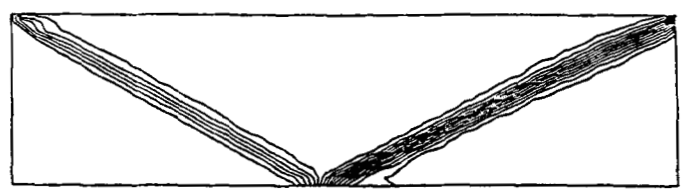

Figure 8. Pressure contours for the wave reflection problem (H^1-method, $\beta = 10^{-6}$, 10×30 8-node quadratic elements, $\Delta t = 0{\cdot}333\,33$, 14 time steps)

4. AN APPROXIMATE 'CONSERVATIVE' FORM

4.1. Formulation

The LSFEM described in Section 2 is based on a non-conservative formulation. Here we would like to construct a conservative LSFEM (in the sense of the steady state). The Euler equations governing two-dimensional compressible inviscid flows can be written in conservative form as

$$\frac{\partial \mathbf{q}}{\partial t} + \frac{\partial \mathbf{F}}{\partial x} + \frac{\partial \mathbf{G}}{\partial y} = \mathbf{0} \qquad \text{in } \Omega \times (0, T), \tag{17}$$

$$\mathbf{M}\mathbf{q} = \mathbf{g} \qquad \text{on } \Gamma_g \times (0, T) \tag{18}$$

$$\mathbf{q} = \mathbf{q}_0 \qquad \text{in } \Omega \text{ for } t = 0, \tag{19}$$

where

$$\mathbf{q} = \begin{bmatrix} \rho \\ \rho u \\ \rho v \\ \rho e \end{bmatrix}, \qquad \mathbf{F} = \begin{bmatrix} \rho u \\ \rho u^2 + p \\ \rho uv \\ (\rho e + p)u \end{bmatrix}, \qquad \mathbf{G} = \begin{bmatrix} \rho v \\ \rho uv \\ \rho v^2 + p \\ (\rho e + p)v \end{bmatrix}, \tag{20}$$

in which e is the total energy and for the case of a perfect gas the equation of state is

$$p = (\gamma - 1)[e - \tfrac{1}{2}\rho(u^2 + v^2)]. \tag{21}$$

Retaining the conservative variables, as an intermediate step we first convert (17) (temporarily) to the following non-conservative form:

$$\frac{\partial \mathbf{q}}{\partial t} + \bar{\mathbf{A}}_1 \frac{\partial \mathbf{q}}{\partial x} + \bar{\mathbf{A}}_2 \frac{\partial \mathbf{q}}{\partial y} = \mathbf{0}, \tag{22}$$

where

$$\bar{\mathbf{A}}_1 = \begin{bmatrix} 0 & 1 & 0 & 0 \\ \frac{1}{2}\bar{\gamma}(u^2 + v^2) - u^2 & (3 - \gamma)u & -\bar{\gamma}v & \bar{\gamma} \\ -uv & v & u & 0 \\ [\bar{\gamma}(u^2 + v^2) - \gamma e]u & \bar{\varepsilon} - \bar{\gamma}u^2 & -\bar{\gamma}uv & \gamma u \end{bmatrix}, \tag{23}$$

$$\bar{\mathbf{A}}_2 = \begin{bmatrix} 0 & 0 & 1 & 0 \\ -uv & v & u & 0 \\ \frac{1}{2}\bar{\gamma}(u^2 + v^2) - v^2 & -\bar{\gamma}u & (3 - \gamma)v & \bar{\gamma} \\ [\bar{\gamma}(u^2 + v^2) - \gamma e]v & -\bar{\gamma}uv & \bar{\varepsilon} - \bar{\gamma}v^2 & \gamma v \end{bmatrix}, \tag{24}$$

in which

$$\bar{\gamma} = \gamma - 1, \qquad \bar{\varepsilon} = \gamma e - \bar{\gamma}\frac{u^2 + v^2}{2}.$$

Using the same procedure as before, we construct a corresponding least-squares weak statement similar to (27) where the matrix operators in (23), (24) are again evaluated at the previous time level. This implies that an approximate conservative form can be reconstructed. Using the relationships

$$\frac{\partial \mathbf{F}^n}{\partial x} = \bar{\mathbf{A}}_1^n \frac{\partial \mathbf{q}^n}{\partial x}, \qquad \frac{\partial \mathbf{G}^n}{\partial y} = \bar{\mathbf{A}}_2^n \frac{\partial \mathbf{q}^n}{\partial y}, \tag{25}$$

we have then a conservative least-squares weak statement: find $\Delta\mathbf{q} \in \mathbf{S} = \{(H^1(\Omega))^4;\ \mathbf{M}(\Delta\mathbf{q}) \le \mathbf{0}$ on $\Gamma_g\}$ such that

$$\int_\Omega \left[\mathbf{v} + \Delta t \bar{\mathbf{A}}_1^n \frac{\partial \mathbf{v}}{\partial x} + \Delta t \bar{\mathbf{A}}_2^n \frac{\partial \mathbf{v}}{\partial y}\right]^{\mathrm{T}} \left[\Delta\mathbf{q} + \Delta t \bar{\mathbf{A}}_1^n \frac{\partial \Delta\mathbf{q}}{\partial x} + \Delta t \bar{\mathbf{A}}_2^n \frac{\partial \Delta\mathbf{q}}{\partial y}\right] \mathrm{d}x\mathrm{d}y$$
$$= -\int_\Omega \left[\mathbf{v} + \Delta t \bar{\mathbf{A}}_1^n \frac{\partial \mathbf{v}}{\partial x} + \Delta t \bar{\mathbf{A}}_2^n \frac{\partial \mathbf{v}}{\partial y}\right]^{\mathrm{T}} \Delta t \left[\frac{\partial \mathbf{F}^n}{\partial x} + \frac{\partial \mathbf{G}^n}{\partial y}\right] \mathrm{d}x\mathrm{d}y \quad \forall\ \mathbf{v} \in \mathbf{S}. \tag{26}$$

Here $\Delta\mathbf{q}$ is the unknown increment in conservative variables for time step Δt. We may use the conservative variables at the previous time step to calculate the nodal values of components of flux $\mathbf{F}^n$ and $\mathbf{G}^n$ and then use a finite element approximation to calculate $\partial\mathbf{F}^n/\partial x$ and $\partial\mathbf{G}^n/\partial y$.

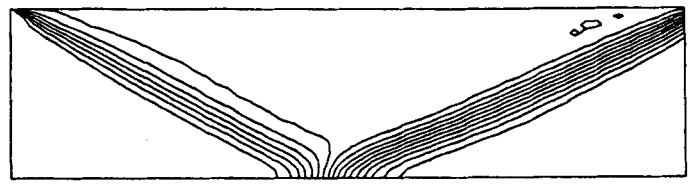

Figure 9. Pressure contours for the wave reflection problem (conservative method, 20×60 bilinear elements, $\Delta t = 0{\cdot}333\,33$, 14 time steps)

4.2. Numerical results

Numerical experiments were conducted with this conservative formulation on the previous shock wave reflection problem and the 20° ramp problem (Problems 1 and 2). The pressure contours for the wave reflection problem are shown in Figure 9. It is observed that there is little difference between the results of non-conservative and conservative LSFEM, except that the results of the conservative method have slight oscillations. The same qualitative comparison also held for the ramp problem.

5. CONCLUSIONS

These exploratory calculations indicate that the method is capable of approximating the shocked flow solution quite well without oscillation or excessive dissipation despite the coarse grid. The L^2-method with linear elements is robust but the shock is somewhat smeared. The H^1-method with quadratic elements has good resolution but includes an added small parameter that must be specified to control shock instabilities. Although the scheme is implicit, the successful use of a large time step and the symmetry of the matrix prove effective for steady state calculations and hence the efficiency is reasonable. Continuing research will be directed towards exploring the limitations of the method and improving its efficiency, as well as the scaling of terms in the objective function.

ACKNOWLEDGEMENTS

This research has been supported in part by the U.T. Hypersonics Program and by the Office of Naval Research. Dr. Jiang also wishes to thank Dr. S. Krishnamachari and Dr. Meng-sing Liou for their constructive comments.

REFERENCES

1. T. J. R. Hughes, 'Recent progress in the development and understanding of SUPG methods with special reference to the compressible Euler and Navier–Stokes equations', *Int. j. numer. methods fluids*, **7**, 1261–1275 (1987).
2. J. Donea, L. Quartapelle and V. Selmin, 'An analysis of time discretization in the finite element solution of hyperbolic problems', *J. Comput. Phys.*, **70**, 463–499 (1987).
3. J. Donea, V. Selmin and L. Quartapelle, 'Finite element schemes for inviscid compressible flows', *Trans. 8th Int. Conf. on Structural Mechanics in Reactor Technology, Vol. B*, North-Holland, 1985, pp. 111–115.
4. A. J. Baker, J. W. Kim, J. D. Freels and J. A. Orzechowski, 'On a finite element CFD algorithm for compressible, viscous and turbulent aerodynamic flows', *Int. j. numer. methods fluids*, **7**, 1235–1259 (1987).
5. J. T. Oden, T. Strouboulis and P. Devloo, 'Adaptive finite element methods for high-speed compressible flows', *Int. j. numer. methods fluids*, **7**, 1211–1228 (1987).
6. R. Löhner, 'FEM–FCT and adaptive refinement schemes for strong unsteady flows', *Int. j. numer. methods fluids*, **7**, 93–114 (1987).

7. J. Peraire, K. Morgan and O. C. Zienkiewicz, 'Convection dominated problems', in T. E. Tezduyar and T. J. R. Hughes (eds), *Numerical Methods for Compressible Flows—Finite Difference, Element and Volume Techniques*, ASME, New York, 1986, pp. 129–148.
8. R. Glowinski and J. Periaux, 'Finite element methods for the compressible Euler and Navier–Stokes equations, application to aerospace engineering', *First World Congr. on Computational Mechanics, Abstracts, Vol. 1*, 1986.
9. K. W. Morton, 'Characteristic Galerkin methods for hyperbolic problems', in *Proc. 5th GAMM Conf. on Numerical Methods in Fluid Mechanics*, Rome, 1983.
10. B. N. Jiang and G. F. Carey, 'Approximation of nonlinear problems by least-squares finite elements', in V. Lakshmikantham (ed.), *Nonlinear Analysis and Application*, Marcel Dekker, New York, 1987.
11. G. F. Carey and B. N. Jiang, 'Least-squares finite elements for first-order hyperbolic systems', *Int. j. numer. methods eng.*, **26**, 81–93 (1988).
12. B. N. Jiang and G. F. Carey, 'A stable least-squares finite element method for first-order hyperbolic systems', *Int. j. numer. methods fluids*, **8**, 933–942 (1988).
13. G. F. Carey and B. N. Jiang, 'Least-squares finite elements for convective transport problems', *Proc. Ninth SPE Symp. on Reservoir Simulation*, Society of Petroleum Engineers (SPE), Inc., 1987, pp. 253–257.
14. G. F. Carey and B. N. Jiang, 'Least-squares finite elements for convective transport problems', *Advances in Water Resources*, submitted.
15. B. N. Jiang and G. F. Carey, 'Least-squares finite elements for compressible Euler equations', in C. Taylor, W. G. Habashi, M. M. Hafez (eds), *Numerical Methods in Laminar and Turbulent Flow, Vol. 5*, Pineridge Press, Swansea, 1987, pp. 1460–1464.